Preprints.org

Article

Not peer-reviewed version

Prediction Equation for Sedimentation Upstream Reservoir of the Weir with Numerical and Experimental Approaches

Jungkyu Ahn , Chang Geun Song , Sung Won Park *

Posted Date: 8 November 2023

doi: 10.20944/preprints202311.0498.v1

Keywords: Sedimentation volume; Laboratory experiments; Unit stream power; Shields parameter; Empirical equation

Preprints.org is a free multidiscipline platform providing preprint service that is dedicated to making early versions of research outputs permanently available and citable. Preprints posted at Preprints.org appear in Web of Science, Crossref, Google Scholar, Scilit, Europe PMC.

Copyright: This is an open access article distributed under the Creative Commons Attribution License which permits unrestricted use, distribution, and reproduction in any medium, provided the original work is properly cited.

Preprints (www.preprints.org) | NOT PEER-REVIEWED | Posted: 8 November 2023 doi:10.20944/preprints202311.0498.v1

Disclaimer/Publisher's Note: The statements, opinions, and data contained in all publications are solely those of the individual author(s) and contributor(s) and not of MDPI and/or the editor(s). MDPI and/or the editor(s) disclaim responsibility for any injury to people or property resulting from any ideas, methods, instructions, or products referred to in the content.

Article

Prediction Equation for Sedimentation Upstream Reservoir of the Weir with Numerical and Experimental Approaches

Jungkyu Ahn [1], Chang Geun Song [2] and Sung Won Park [1,*]

[1] Department of Civil and Environmental Engineering, Incheon National University, Incheon 22012, South Korea; ahnjk@inu.ac.kr

[2] Department of Safety Engineering, Incheon National University, Incheon 22012, South Korea; baybreeze119@inu.ac.kr

* Correspondence: billy1006@gmail.com; Tel.: +82-32-835-8466

Abstract: In this study, a new empirical equation was established to predict the sedimentation volume resulting from the construction of a multipurpose weir or low-head dam. The study employed a one-dimensional numerical model (STAFF) to investigate the key parameters affecting sedimentation volume. Short-term predictions were conducted through laboratory experiments with movable bed, and the results indicated that dimensionless unit stream power and the Shields parameter exhibited the most significant correlation with dimensionless deposition volume. Using a multiple regression approach, an empirical equation was formulated and validated for predicting sedimentation in the upstream reservoir of the weir.

Keywords: sedimentation volume; laboratory experiments; unit stream power; shields parameter; empirical equation

1. Introduction

The dredging of river channels has been a common practice in the construction of low-head dams and multi-purpose weirs, where these hydraulic structures are designed to manage water flow and sediment movement patterns. However, such installations have led to significant alterations in the flow patterns of rivers and the transport of sediments. As a consequence, changes in sedimentation and erosion patterns within the river channel have become apparent. Over the medium to long term, this has resulted in modifications to the characteristics of the riverbed material, the cross-sectional shape of the river, and the slope of the riverbed. Furthermore, the management of water levels and flow control associated with multi-functional weirs have introduced an additional factor known as the backwater effect. This effect gradually gives rise to the formation of a reservoir delta. The reservoir delta is a distinct landform that emerges from the rapid deposition of sediment transported downstream, particularly in areas where water depths are higher, and flow velocities slow down due to the influence of hydraulic structures such as dams and weirs, which induce backwater conditions [1,2]. Reservoir deposition changes through a very complex process depending on sediment discharge generated from the river basin, transportation capacity, bed form, etc. In particular, it is mainly influenced by flood frequency, reservoir topographical characteristics and operation, cohesion capacity, density flow, and land use changes, and should be analyzed taking into account dead zone, trap efficiency, hydrograph of upstream, sediment discharge [3]. The topographical features of a reservoir delta typically consist of three key elements: a topset bed composed of coarse pseudo-particles, a foreset bed forming a steep slope, and a bottomset bed characterized by silt or fine particles. The formation of this reservoir delta occurs when sediment-laden water from upstream meets the reservoir, causing a sharp reduction in flow velocity. This phenomenon results in a decrease in the effective storage capacity of the reservoir and an increase in the flood level of the river, thereby aggravating flood damages during the rainy season [3]. While in

© 2023 by the author(s). Distributed under a Creative Commons CC BY license.

Preprints (www.preprints.org) | NOT PEER-REVIEWED | Posted: 8 November 2023 doi:10.20944/preprints202311.0498.v1

the short term, a reservoir delta may not bring about significant topographical changes, its long-term effects can be substantial. These effects include a notable reduction in the cross-sectional area and storage capacity of the river, leading to issues such as the expansion of flood inundation and a decline in the reliability of stable water supply. Moreover, the sedimentation of reservoirs poses a threat to the safety of river embankments and hydraulic structures, impacting the operation and management of river facilities. Globally, it is well-documented that the storage capacity of dams decreases at an annual rate of approximately 0.5 to 1.0% due to sedimentation [4]. Additionally, Toniolo and Parker [5] have analyzed that the presence of reservoir deltas causes an annual decrease of about 1% in reservoir capacity [5].

In recent years, there has been a growing focus on issues related to reduced storage capacity due to sediment deposition and increased flood levels. Numerous researchers are actively investigating these challenges. Research into numerical modeling approaches for studying sediment deposition in natural rivers can be categorized based on the dimensionality of the numerical models employed. Among these approaches, 3-D numerical models are often employed to examine short-term variations in the movable bed, particularly in the vicinity of hydraulic structures such as piers, upstream of outfalls, and directly downstream of multi-purpose weirs. While these models are valuable for short-term predictions, conducting long-term predictions for relatively long-term periods demands substantial effort and time. To develop effective sediment management plans for areas upstream of weirs, it is imperative to comprehend the deposition mechanisms of reservoir deltas. Various empirical research methods and numerical analysis techniques have been employed to predict sediment deposition upstream of dams or reservoirs. Wright and Coleman [6] conducted field research along the Mississippi River in the United States, categorizing reservoir delta shapes into distal bars, bar backs, bar crests, and bar fronts.

Soni et al. [7], Hotchkiss [8], and Hotchkiss and Parker [9] conducted mathematical model experiments and numerical analyses to evaluate the applicability of one-dimensional numerical models for sediment transport. One-dimensional models for bed elevation change were well-suited for conducting numerical analyses over extended time periods [1,10–12]. Fan and Morris [13,14] analyzed data collected before and after flood events, as well as discharge-related data, with a focus on bed elevation changes in the Sanmenxia Reservoir within the Yellow River basin of China. Ahn et al. [15] utilized a one-dimensional model, GSTARS, to predict reservoir sedimentation and evaluate changes in riverbed conditions pre- and post-discharge events. This research collectively contributes to our understanding of sediment dynamics and hydraulic behavior in river systems. Choi [16] implemented laboratory experiments with mobile bed and validated empirical equation to predict sediment deposition.

Within the realm of sediment deposition in reservoirs, several experimental and field studies have provided valuable insights. In an experimental context, KanToush et al. [17] conducted hydraulic experiments and numerical analyses to investigate deposition in channels with rectangular cross-sections. Gökçen and Güney [18] carried out hydraulic experiments and subsequently applied previously established empirical equations to assess their impact on sediment transport, thoroughly analyzing the key influencing parameters. Matthieu et al. [19] developed an empirical equation by scrutinizing the relationship between reservoir deposition and critical parameters, including channel width, dimensionless length, and water depth, through hydraulic model experiments. Souza et al. [20] explored the prediction of deposition mechanisms via a combination of mathematical experiments and numerical analysis. Notably, there has been a growing expansion of numerical analysis studies in tandem with advancements in computing resources [21]. Moreover, efforts to enhance our understanding of the time series patterns associated with sediment transport mechanisms have been underway. This includes the application of neural network and machine learning technologies, as evidenced by the work of Latif et al. [22]. These endeavors collectively contribute to the ongoing refinement of our knowledge within the field of river mechanics and hydraulics.

The primary objective of this research is to investigate the volume and spatial distribution of sediment deposition upstream of a weir through experimental studies. The study aims to examine

Preprints (www.preprints.org) | NOT PEER-REVIEWED | Posted: 8 November 2023 doi:10.20944/preprints202311.0498.v1

the relationship among key parameters such as sediment particle size, bed slope, flow velocity, and water depth, which interactively influence sediment deposition mechanism. To achieve this goal, a one-dimensional numerical analysis model was employed to analyze these parameters, ultimately leading to the derivation of an empirical equation for predicting sediment deposition volume. The developed equation was rigorously tested and validated against experimental results to ensure its accuracy and reliability.

2. Theoretical Backgrounds

2.1. Reservoir Delta Theory

Backwater forms in reservoirs located upstream of hydraulic structures, such as dams or multi-purpose weirs, which serve various functions like flood control and water supply. When the flow entering into this backwater section increases, it results in an expansion of the passage area and a subsequent decrease in flow velocity and turbulence. Consequently, the sediment transport capacity decreases, causing sediments from upstream to settle at the reservoir's bottom. In this process, coarser sediments, such as gravel and sand, tend to preferentially deposit at the reservoir inlet, gradually forming what is known as a reservoir delta. On the other hand, fine particles like silt and clay pass through the reservoir delta in the form of density flow and subsequently settle within the reservoir. It's worth noting that if the inflowing sand from the basin contains a significant proportion of fine particles, the impact of fine particle deposition due to density currents on the reduction of reservoir capacity may not be substantial.

Sediment deposition within the reservoir occurs gradually over a specific period during the operation of a weir or dam. As the river's flow diminishes, coarse materials accumulate in the impounded water, primarily in the upstream section of the reservoir. The transportation of bed load is driven by the movement of water waves. In this study, the concept of a reservoir delta, as depicted in Figure 1, is introduced to analyze the behavior of the reservoir delta upstream of the weir in response to the presence of a multi-purpose weir [23].

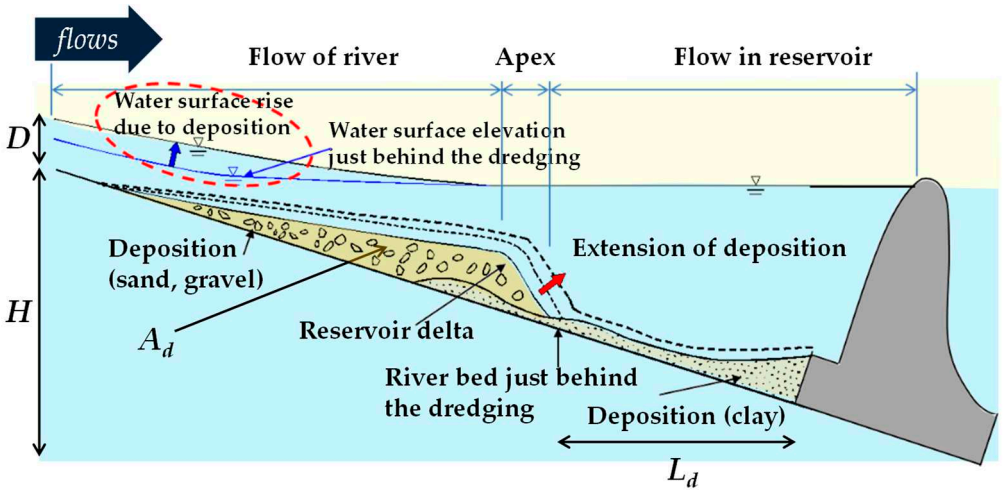

Figure 1. Schematic diagram of reservoir delta deposition at the upstream of weir gate.

Variables in Figure 1 are defined as follows: A_d represents the sediment load amount per unit width, and L_d indicates the distance from the main body of the multi-purpose weir to the starting point of the reservoir delta. To analyze the behavior of sediment particle erosion and deposition, dimensionless variables were introduced, as illustrated in Figure 2.

Preprints (www.preprints.org) | NOT PEER-REVIEWED | Posted: 8 November 2023 doi:10.20944/preprints202311.0498.v1

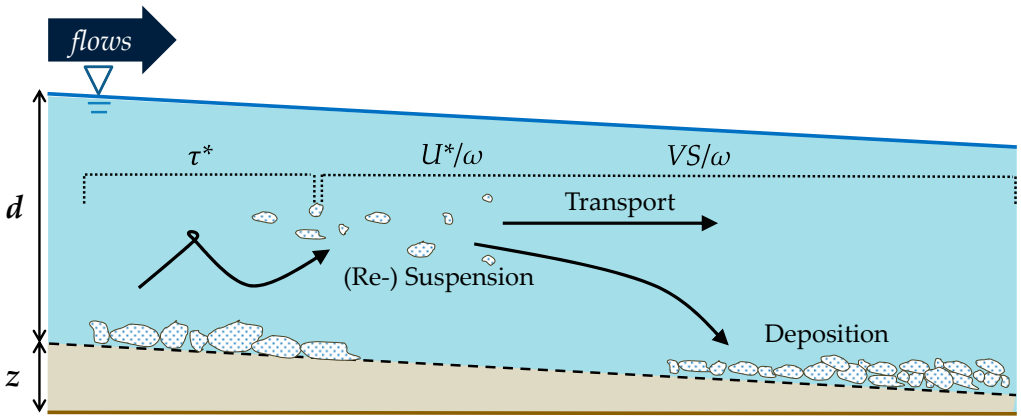

Figure 2. Schematic diagram of reservoir sedimentation and dimensionless.

In Figure 2, the concept of VS/ω is an extension of VS (Unit Stream Power) originally proposed by Yang [24]. It represents the rate of energy dissipation of water per unit weight divided by the fall velocity (ω) of sediment particle. And V and S denote the flow velocity and the river bed slope, respectively. U^*/ω represents the ratio of the friction velocity applied to sediment particles and the fall velocity acting in the direction of gravity, and the delivery and deposition of sediment particle can be determined according to U^*/ω.

$$U^* = \sqrt{gRS} \tag{1}$$

$$\tau^* = \frac{\tau_0}{\gamma(G-1)d_s} \tag{2}$$

where, U^* = the friction velocity; g = gravitational acceleration (= 9.81 m/s^2); R= hydraulic radius; τ^* = the Shields parameter; τ_0 = bed shear stress; γ= specific weight of water; G= specific gravity of sediment; and d_s= sediment particle size. It should be noted that the Shields parameter can be calculated based on particle size and unit weight of sediment, and the shear velocity of the particle, as previously defined by Shields [25]. The Shields parameter is utilized in the analysis of incipient motion criteria for sediment particles and the assessment of changes in riverbed morphology. It is defined in Equation (2) as a dimensionless variable that corresponds to the vertical axis of the Shields diagram.

This study primarily focuses on the computation of one-dimensional sedimentation patterns and sediment deposition amounts (A_d) to examine the sedimentation pattern of a reservoir delta. To achieve this, a combination of numerical analysis using a one-dimensional numerical model and mobile bed experiments was conducted. The objective was to reveal relationships between dimensionless deposition per unit width (A_d/qt) and dimensionless variables such as dimensionless unit stream power (= VS/ω), the Shields parameter (= τ^*), and U^*/ω. The aim was to investigate and comprehend these relationships thoroughly.

2.2. Model Description

HEC-RAS, GSTARS, and Fluvial-12, which are widely utilized one-dimensional numerical simulation for bed elevation change and sediment transport modeling, employ an un-coupled scheme. This scheme calculates hydraulics and sediment routing processes, separately. The numerical analysis technique utilized in this study also employs the uncoupled scheme akin to a standard one-dimensional bed elevation change model. The process commences with hydraulic analysis, which uses defined upstream and downstream boundary conditions to compute hydraulic parameters such as flow velocity, water depth, bottom shear stress, and friction slope. Subsequently, these hydraulic parameters are employed to calculate sediment transport. Finally, bed elevation change can be calculated. The bed elevation change is then updated, and the model progresses to the next time step, repeating the same sequence of calculations. These approaches are referred to as

Preprints (www.preprints.org) | NOT PEER-REVIEWED | Posted: 8 November 2023 doi:10.20944/preprints202311.0498.v1

STAFF (Sediment Transport Analysis For Flume) model, and its detailed descriptions are given as follows.

1. Flow velocity

Using the energy equation given as follows:

$$h_2 + \beta_2 \frac{V_2^2}{2g} = h_1 + \beta_2 \frac{V_1^2}{2g} + h_L \tag{3}$$

where, subscripts 1 and 2 denote the downstream and upstream, respectively; h= water surface elevation; β= energy coefficient (≈ 1); and h_L= energy loss. Assuming that h_L is initiated by bottom friction, it can be expressed as the arithmetic average of the upper and lower cross sections as follows:

$$h_L = \frac{1}{2}(S_{f2} + S_{f1})\Delta x \tag{4}$$

where, S_f= friction slope; and Δx= stream-wise distance. Equation (4) can be rewritten with Equation (3) as:

$$h_2 = h_1 + \frac{V_1^2}{2g} - \frac{V_2^2}{2g} + \frac{1}{2}(S_{f2} + S_{f1})\Delta x \tag{5}$$

Since this study focused on simulating the two-dimensional (stream- & depth-wise direction) behavior of a rectangular cross-section, the following relationship can be satisfied.

$$\frac{V_2^2}{2g} = \frac{q^2}{2gd_2^2} = \frac{q_2^2}{2g(h_2 - Z_2)^2} \tag{6}$$

$$\frac{V_1^2}{2g} = \frac{q^2}{2gd_1^2} = \frac{q_1^2}{2g(h_1 - Z_1)^2} \tag{7}$$

where, q= discharge per unit width; d= water depth; and Z= bed elevation from datum. Using Manning's roughness equation:

$$S_{f2} = \frac{n^2 q^2}{(h_2 - Z_2)^{\frac{10}{3}}} \tag{8}$$

$$S_{f1} = \frac{n^2 q^2}{(h_1 - Z_1)^{\frac{10}{3}}} \tag{9}$$

where, n= the Manning's roughness coefficient. Substituting Equation (6) – (9) into Equation (5) yields

$$\begin{aligned} f(h_2) = h_2 - h_1 - \frac{q_1^2}{2g(h_1 - Z_1)^2} + \frac{q_2^2}{2g(h_2 - Z_2)^2} \\ - \frac{1}{2}\left[\frac{n^2 q^2}{(h_2 - Z_2)^{10/3}} + \frac{n^2 q^2}{(h_1 - Z_1)^{10/3}}\right]\Delta x = 0 \end{aligned} \tag{10}$$

The STAFF model calculates h_2 using the Newton-Raphson method when h_1 is given.

2. Sediment load

In this study, sediment concentration was calculated using the Engelund-Hansen formula [26].

$$C_w = 0.05\left(\frac{G}{G-1}\right)\frac{VS_f}{[(G-1)gd_s]^{1/2}}\left[\frac{dS_f}{(G-1)d_s}\right]^{1/2} \tag{11}$$

where, C_w= sediment concentration by weight. C_v (= sediment concentration by volume) can be rewritten as follows:

$$C_v = \frac{C_w}{G - (G-1)C_w} \tag{12}$$

Also, sediment discharge per unit width, q_s, can be calculated as follows:

Preprints (www.preprints.org) | NOT PEER-REVIEWED | Posted: 8 November 2023 doi:10.20944/preprints202311.0498.v1

$$q_s = C_v \cdot V \cdot d_s \tag{13}$$

3. Bed elevation change

Research on predicting bed elevation change according to the flow of water in natural rivers began when Exner [27] first introduced the continuity equation with the concept that the mass of water and sediment is conserved. Assuming that it is a one-dimensional flow in which the riverbed moves and that there is no lateral inflow, the Exner equation can be rewritten as follows:

$$(1-p)\frac{\partial Z}{\partial t} = -\frac{\partial q_s}{\partial x} \tag{14}$$

where, p= porosity of soil; t= time; and x= stream-wise length. Differencing Equation (14) with FTBS (Forward in Time Backward in Space) scheme:

$$\Delta Z_j^k = Z_j^{k+1} - Z_j^k = -\frac{1}{(1-p)}\frac{\left(q_{s_j}^{\ k} - q_{s_{j-1}}^{\ k}\right)\cdot \Delta t}{\Delta x} \tag{15}$$

where, ΔZ= bed elevation change; Δt= time step; and j & k= spatial and temporal index. The calculation procedure (hydraulic variables for steady flow, sediment load, bed elevation change) described in chapter 2.2.1 is shown in Figure.

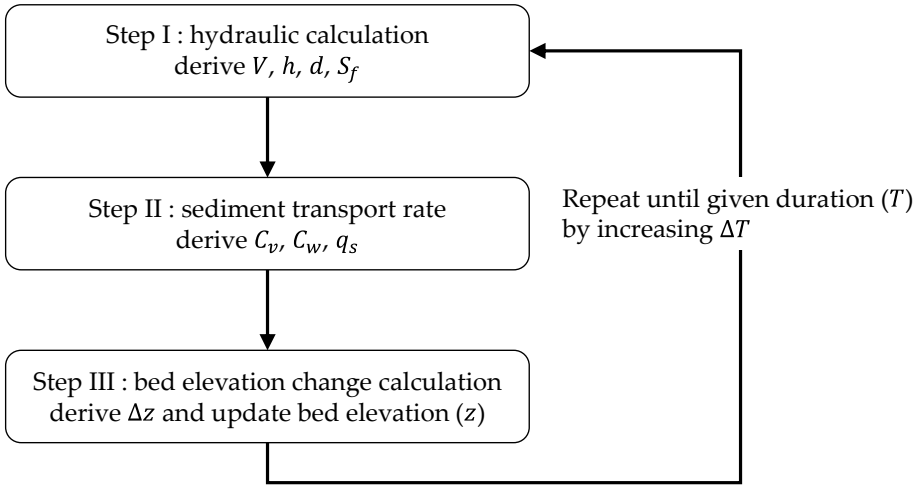

Figure 3. Flow chart of STAFF model calculation.

3. Laboratory Experiments

3.1. Dimensional analysis

Dimensional analysis was performed to analyze the factors affecting the sedimentation amount. Representative factors affecting A_d are as follows:

$$A_d = f(\rho, \nu, H, D, S, d_s, \omega, g, V, U^*, t) \tag{16}$$

where, ρ= density of fluid; ν= kinematic viscosity; and D = upstream normal depth. Rewriting Equation (16) for performing the standard dimensional analysis:

$$\frac{A_d}{qt} = f(\mathrm{Re}, \mathrm{Fr}, \frac{\omega t}{D}, \frac{D}{d_s}, \frac{VS}{\omega}, \frac{U^*}{\omega}, \tau^*, \frac{H}{D}) \tag{17}$$

As the experimental flow condition in this study represents fully turbulent flow, excluding the Re & Fr to assess the impact of viscosity on bed elevation changes, the sensitivity analysis was performed on the remaining six dimensionless parameters.

Preprints (www.preprints.org) | NOT PEER-REVIEWED | Posted: 8 November 2023 doi:10.20944/preprints202311.0498.v1

3.2. Model simulitude

River hydraulics research can be categorized into two main types: (1) researches focusing on water level and flow rate within the channel; and (2) researches concentrating on sediment transport and bed elevation changes. The former typically employs a fixed bed model, while the latter involves a mobile bed model. When conducting hydraulic model experiments using a scaled-down model to understand the hydraulic behavior occurring in natural rivers, as is the case in this study, it's essential to ensure hydraulic similitude between the flow behavior in the prototype and the scaled model. Generally, in hydraulic experiments, Froude similitude and Reynolds similitude are the primary similitudes applied. However, in mobile bed experiments, achieving ideal conditions for these variables can be challenging due to issues such as spatial constraints and limitations in implementing sediment particles. Consequently, in this study, experimental conditions were devised to meet the similitude for sediment discharge by applying the Exner equation, which served as the governing equation for the analysis of bed elevation changes.

Equation (14) can be expressed as follows:

$$\Delta Z = \frac{1}{1-p}\frac{\Delta q_s}{\Delta x}\Delta t \tag{18}$$

To satisfy hydraulic similitude, Equation (18) can also be expressed with conversion ratio between prototype and scaled model as follows:

$$t_r = (1-p)_r X_r Z_r q_{sr}^{-1} \tag{19}$$

where, subscript sr= scale ratio between prototype and scaled model; X_r, and Z_r= scale ratios for horizontal and vertical direction, respectively; and q_{sr}= scale ratio of sediment load per unit width. q_{sr} in Equation (19) can be calculated through the scale ratio of q_{sp} and q_{sm} as follows. Sediment load per unit width can be calculated using the sediment transport formula proposed by Yang [28]. It was assumed that the amount of sediment in a river is related to the dissipation rate of the potential energy of water, and if the potential energy of a river decreases by Δz at Δt, its dissipation rate is as follows:

$$\frac{\Delta z}{\Delta t} = \frac{\Delta x}{\Delta t}\frac{\Delta z}{\Delta x} = VS \tag{20}$$

In this context, Yang [28] introduced the concept of unit stream power, defining it as the power of water per unit weight. Yang developed an equation using existing sediment transport data with unit stream power as a variable, which is as follows:

$$\begin{aligned}\log C_t = {} & 5.435 - 0.286\log\frac{\omega d_s}{\nu} - 0.457\log\frac{U^*}{\omega} \\ & + \left(1.799 - 0.409\log\frac{\omega d_s}{\nu} - 0.314\log\frac{U^*}{\omega}\right)\times\log\left(\frac{VS}{\omega} - \frac{V_c S}{\omega}\right)\end{aligned} \tag{21}$$

where, C_t= sediment concentration in parts per million by weight; V_c (= critical average flow velocity in incipient motion) can be calculated with following Equation (22):

$$\frac{V_c}{\omega} = \begin{cases} \dfrac{2.5}{\log(U^* d_s/\nu - 0.06)} + 0.66 \; ; 1.2 < \dfrac{U^* d_s}{\nu} < 70 \\ 2.05; \dfrac{U^* d_s}{\nu} \geq 70 \end{cases} \tag{22}$$

Procedure to estimate total sediment load using Yang's formula [28] is as follows:

- Estimate VS, $\omega d_s/\nu$, U^*/ω from prototype and scaled model, respectively.
- Calculate particle Reynolds number (= $U^* d_s/\nu$) and V_c/ω in Equation (22).
- Calculate C_t using Equation (21) and Q_s using discharge.

3.3. Numerical results of STAFF model

Due to limitations in experimental conditions, numerical simulations were performed for a total of 2,646 conditions with respect to various discharges and sediment particle sizes in a range that

Preprints (www.preprints.org) | NOT PEER-REVIEWED | Posted: 8 November 2023 doi:10.20944/preprints202311.0498.v1

could not be reproduced by laboratory experiments. Figure 4 shows the relationship between A_d and dimensionless variables.

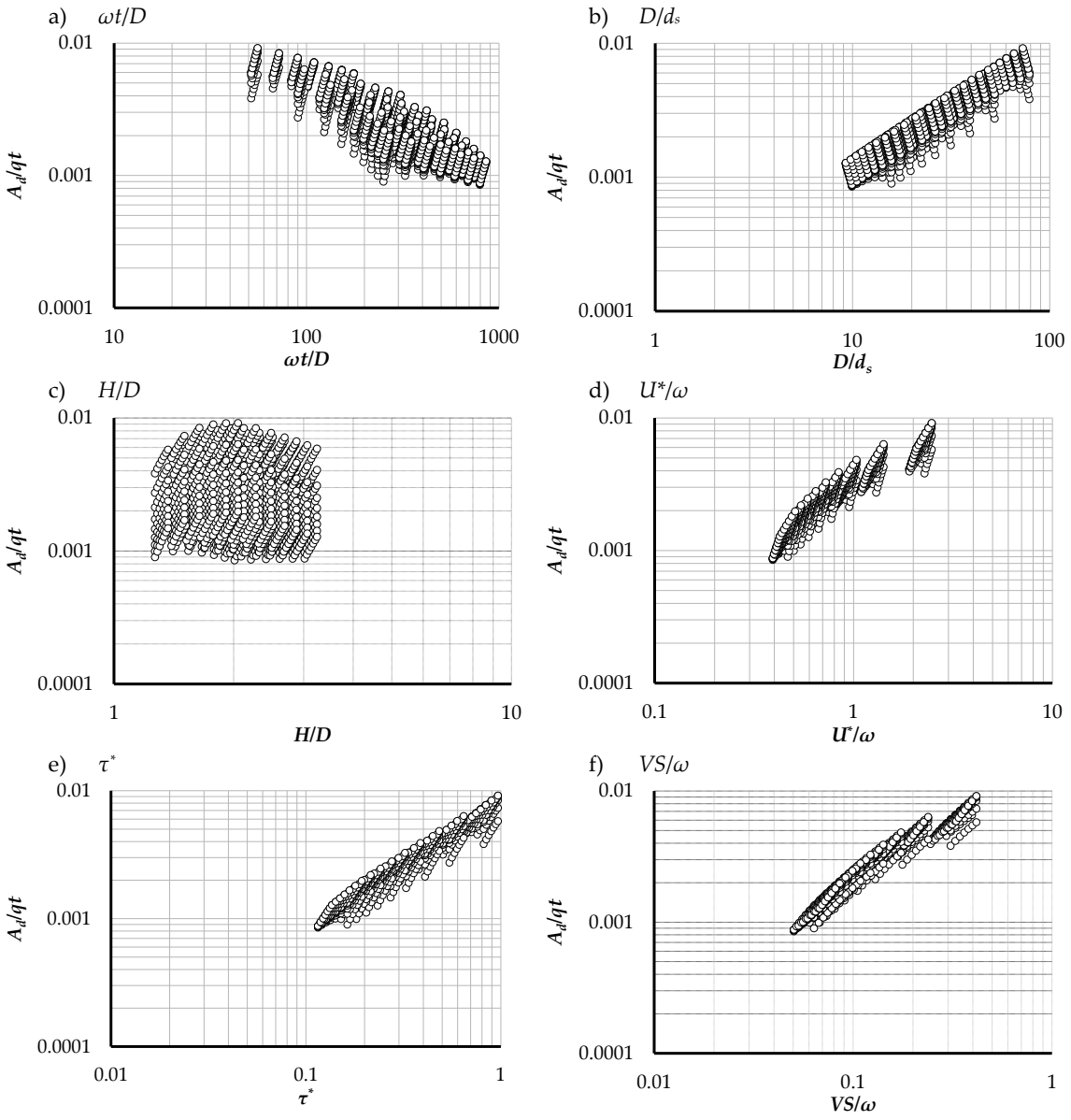

Figure 4. Results of STAFF model (2,646 cases).

As shown in Figure 4, A_d/qt showed a large correlation in the order of dimensionless unit stream power, shields parameter, U^*/ω, and D/d_{50}. Consequently, in the laboratory experiment, it was decided to measure and analyze VS/ω, τ^*, U^*/ω, and D/d_{50}.

3.4. Experimental setup and measuring apparatus

Sediment Channel-I (SC-I) is a flume of rectangular cross-section with dimensions of 78 mm in width, 1,550 mm in length, and 110 mm in height. This flume offers the flexibility to apply various experimental conditions by adjusting the slope of the flume using a slope control device, allowing the bed slope to closely match that of natural rivers. At the downstream end of the flume, a multi-purpose weir model with adjustable height was manufactured and installed. It was modified to facilitate hydraulic model experiments in accordance with multi-purpose weir management water level operation (Figure 5).

a) Side view of whole channel (schematic)

Preprints (www.preprints.org) | NOT PEER-REVIEWED | Posted: 8 November 2023 doi:10.20944/preprints202311.0498.v1

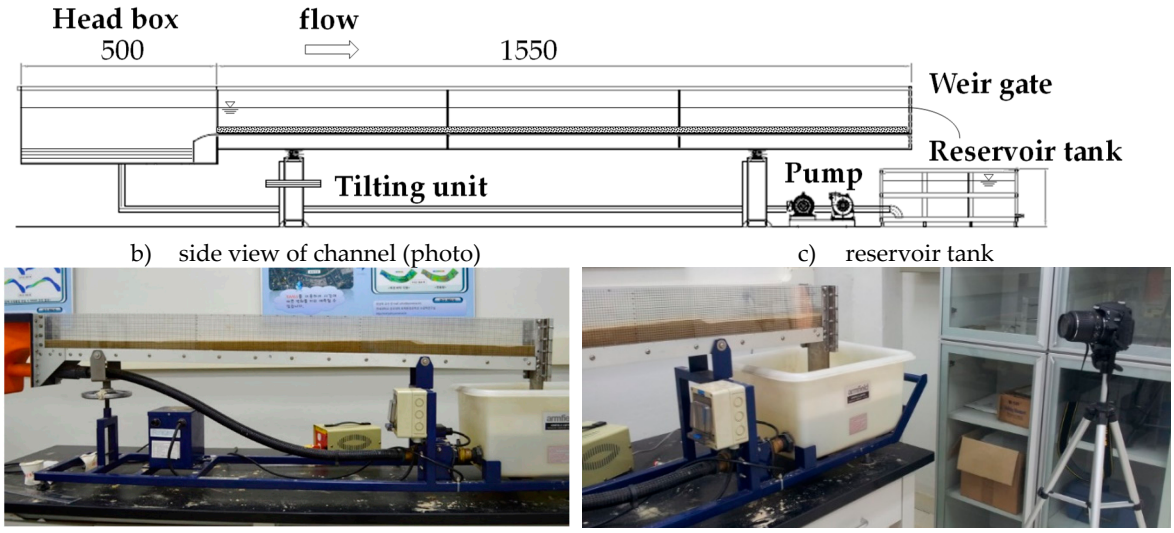

Figure 5. Experimental sediment channel-I (SC-I) and its arrangement.

The sediment channel-II (SC-II) is a flume with dimensions of 300 mm wide, 10,000 mm long, and 600 mm high. It was equipped with a slurry pump capable of circulating sediment particle. The inlet discharge range is from 0.6 to 8.0 liters per second, and similar to SC-I, the flume's slope can be finely adjusted in the vertical direction up to 500 mm. At the downstream part, a fixed weir model was installed to maintain the water level consistent. Additionally, an upstream stabilizer with dimensions of 295 mm in width, 600 mm in length, and 100 mm in height was installed to prevent unexpectedly rapid erosion of the mobile bed by the flow originating from the head tank (Figure 6).

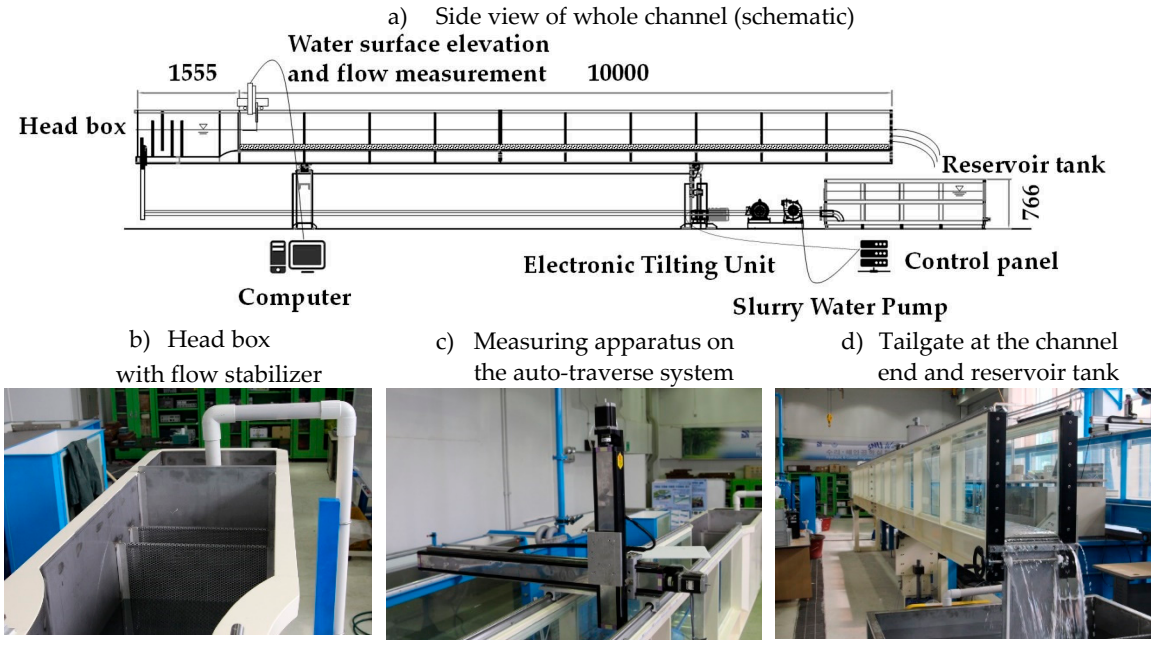

Figure 6. Experimental channel (SC-II) and setup.

3.5. Experimental procedure and condition

In the SC-I experimental conditions, mobile bed experiments were conducted using three different sediment particles (with d_{50} = 0.20, 0.62, and 1.20 mm). Also, d_s was replaced by median grain size, d_{50} for the uniform particle. A 5 mm scale was affixed to the right glass wall of the flume, spanning a section of 1,550 mm. Images were captured at 30-second intervals using a Digital Single Lens Reflex (DSLR) camera, allowing for the determination of water surface elevation under various

Preprints (www.preprints.org) | NOT PEER-REVIEWED | Posted: 8 November 2023 doi:10.20944/preprints202311.0498.v1

experimental conditions through image processing. Bed elevation was also measured at each time step.

In the case of the SC-II experiment, the adjustable slope system was designed to allow for slope adjustment within the range of 0% to 2.38%. At the downstream part, a fixed tailgate was installed to control the water depth. Sediment particle (d_{50}= 0.62 mm) was used, and for each experimental condition, the sediment was placed at a height of 100 mm from the floor, covering a 10,000 mm section of the test water. The experiment had a duration of 9 minutes, and measurements of bed elevation and water depth were taken at five times: 1, 3, 5, 7, and 9 minutes later each. The experiment commenced as soon as flow was introduced to the experimental waterway, precisely when backwater was initiated at the downstream end [29].

4. Results and Analysis

4.1. Experimental results

Based on the experimental conditions presented in Table 1, changes in bed elevation and water depth over time are graphically shown (Figure 7). The initial bed profile is depicted with a bold line, and the upper lines without markers and the lower lines with markers represented the water surface elevation and bed elevation profiles for each time step, respectively. The experiment under the condition of d_{50}= 0.20 mm was conducted for 4 minutes each, and bed elevation and water depth were measured every minute to analyze variations of them over time. The scenario in which the water depth at the downstream end was 20 mm and the channel slope varied from 2.2% to 3.1% led to an expansion of the reservoir delta by approximately 50 mm in the stream-wise direction and an increase in bed elevation of about 4 mm in the depth-wise direction, as depicted in Figure 7a & c. Moreover, in the scenario where the water depth downstream was 30 mm and the channel slope also varied from 2.2% to 3.1%, it resulted in the expansion of the reservoir delta by approximately 250 mm in the stream-wise direction and 5 mm depth-wise direction (Figure 7b & 7d). Second, in a scenario where H = 30 mm and values of S changes to the same as the H = 20 mm condition, the reservoir delta grows by about 250 mm in the stream-wise direction and 5 mm in the depth-wise direction (Figures 7b & 7d). Through mass conservation calculations, it was confirmed that A_d increased by approximately 3.4 times, growing from 1,500 mm² to 5,100 mm² as the slope increased from 2.2% to 3.1%, as shown in Figure 7.

Table 1. Experimental conditions and parameters.

Types	No. of Cases	S (-)	Q (l/sec)	H (mm)	d_{50} (mm)	D/d_{50}	U^*/ω	τ^*	VS/ω
SC-**I** tests	288	2.2-4.0	0.215 -0.368	20-30	0.20 -1.20	2.5 -75.0	0.315 -2.456	0.0606 -1.1879	0.0796 -0.6496
SC-**II** tests	30	0.8-2.0	3-6	100	0.62	25.8 -45.2	0.488 -0.905	0.1251 -0.4301	0.0021 -0.0188

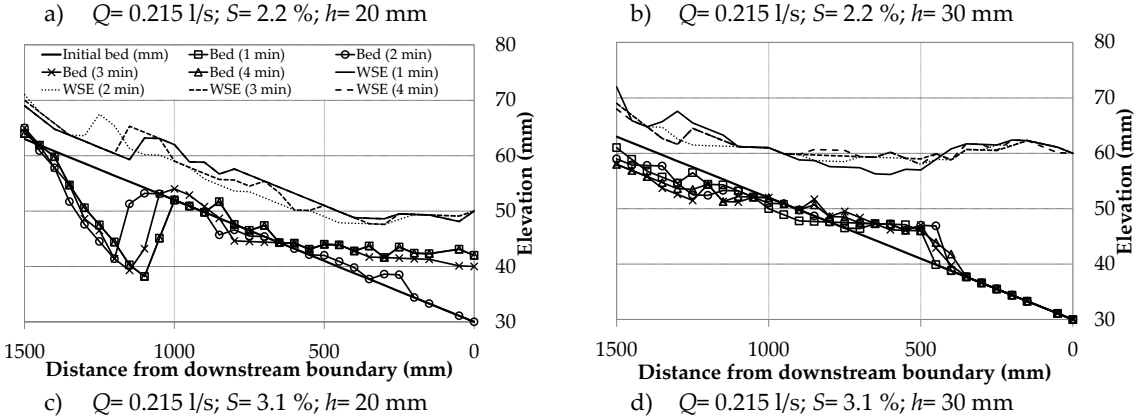

Preprints (www.preprints.org) | NOT PEER-REVIEWED | Posted: 8 November 2023 doi:10.20944/preprints202311.0498.v1

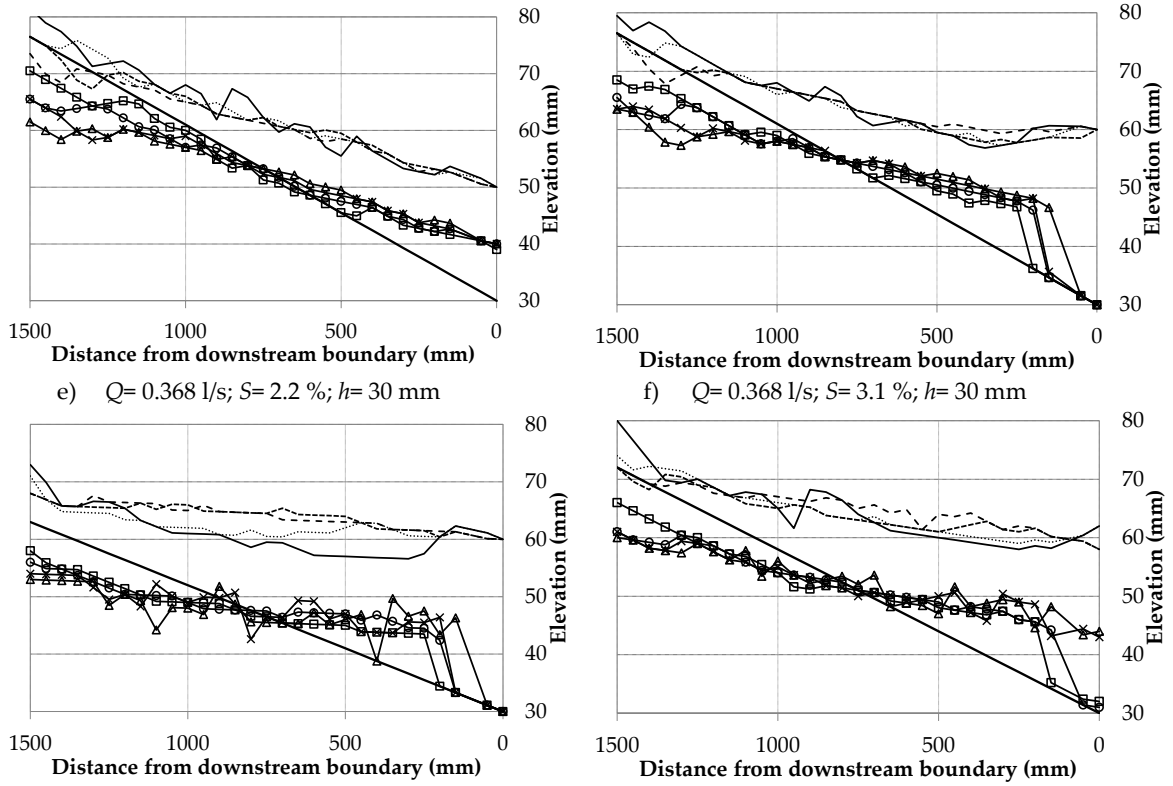

e) Q= 0.368 l/s; S= 2.2 %; h= 30 mm

f) Q= 0.368 l/s; S= 3.1 %; h= 30 mm

Figure 7. Comparison of delta deposition of SC-I experiments with d_{50}= 0.20 mm.

Temporal change of bed elevation profiles in the case with d_{50} = 0.62 mm were analyzed in a manner similar to that in the case with d_{50} = 0.20 mm. In other words, in the case of the minimum channel slope (=2.2%), the sediment deposition per unit width was calculated to be 3,450 mm², while for the maximum channel slope (= 3.1%), A_d was estimated to be 7,300 mm², which is about 3.4 times larger (Figure 8).

For the case with d_{50} = 1.2 mm under the experimental conditions, A_d had a trend to increase by about 40% as the river bed slope increased by 0.2%. Notably, lower downstream water depth resulted in a shorter period for the creation of the reservoir delta and a quicker decline in reservoir capacity (Figure 9). And, in the case of the d_{50} = 0.2 mm series under same experimental conditions, A_d increased by about 1.8 times as the flow discharge rose from 0.215 l/s to 0.368 l/s. However, for the series with similar particle size (d_{50} = 1.2 mm), A_d increased by approximately 2.6 times under the same experimental conditions, indicating that the series with a larger sediment particle was more sensitive to changes in flow rate compared to the series with a smaller sediment particle (Figure 9). The overall relationship between A_d and L_d versus S were plotted and compared in Figure 10.

a) Q= 0.215 l/s; S= 2.2 %; h= 20 mm

b) Q= 0.215 l/s; S= 2.2 %; h= 30 mm

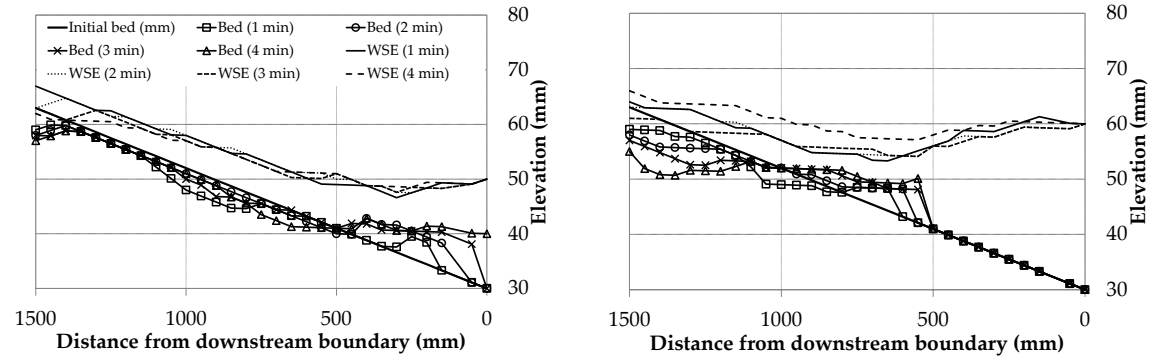

c) Q= 0.215 l/s; S= 3.1 %; h= 20 mm

d) Q= 0.215 l/s; S= 3.1 %; h= 30 mm

Preprints (www.preprints.org) | NOT PEER-REVIEWED | Posted: 8 November 2023 doi:10.20944/preprints202311.0498.v1

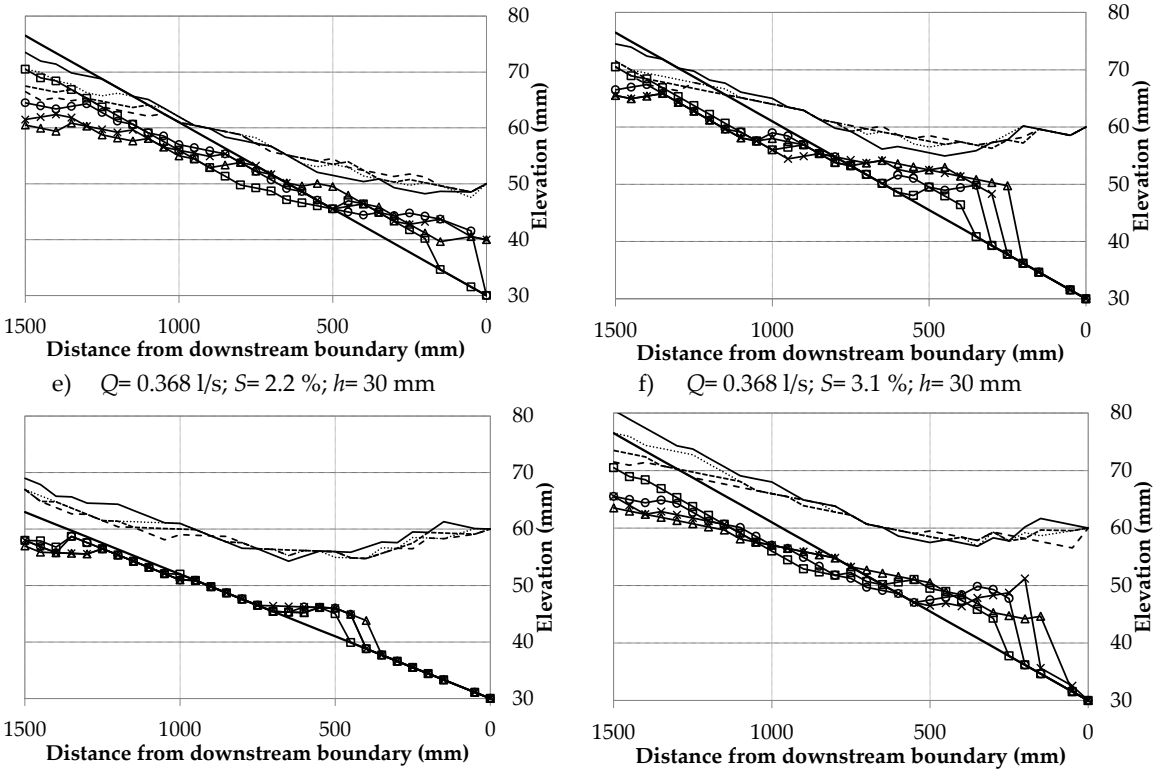

e) Q= 0.368 l/s; S= 2.2 %; h= 30 mm

f) Q= 0.368 l/s; S= 3.1 %; h= 30 mm

Figure 8. Comparison of delta deposition of SC-I experiments with d_{50}= 0.62 mm.

a) Q= 0.215 l/s; S= 2.2 %; h= 20 mm

b) Q= 0.215 l/s; S= 2.2 %; h= 30 mm

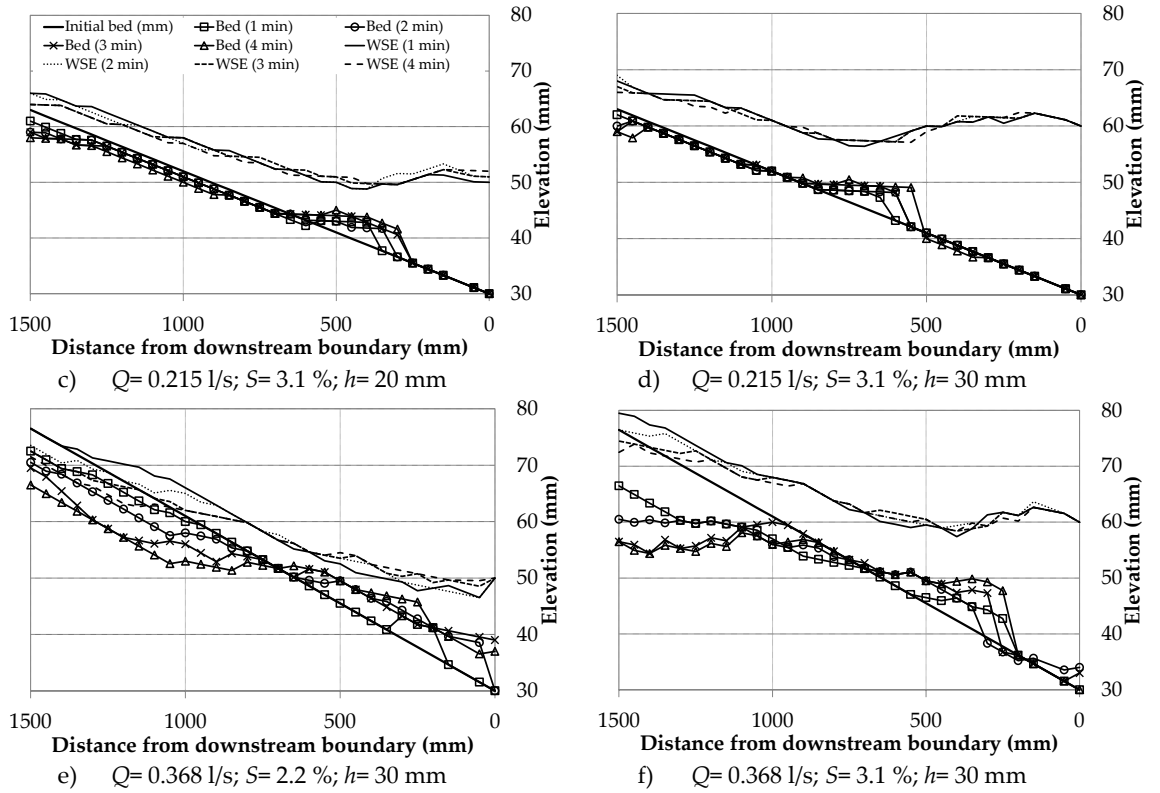

c) Q= 0.215 l/s; S= 3.1 %; h= 20 mm

d) Q= 0.215 l/s; S= 3.1 %; h= 30 mm

e) Q= 0.368 l/s; S= 2.2 %; h= 30 mm

f) Q= 0.368 l/s; S= 3.1 %; h= 30 mm

Preprints (www.preprints.org) | NOT PEER-REVIEWED | Posted: 8 November 2023 doi:10.20944/preprints202311.0498.v1

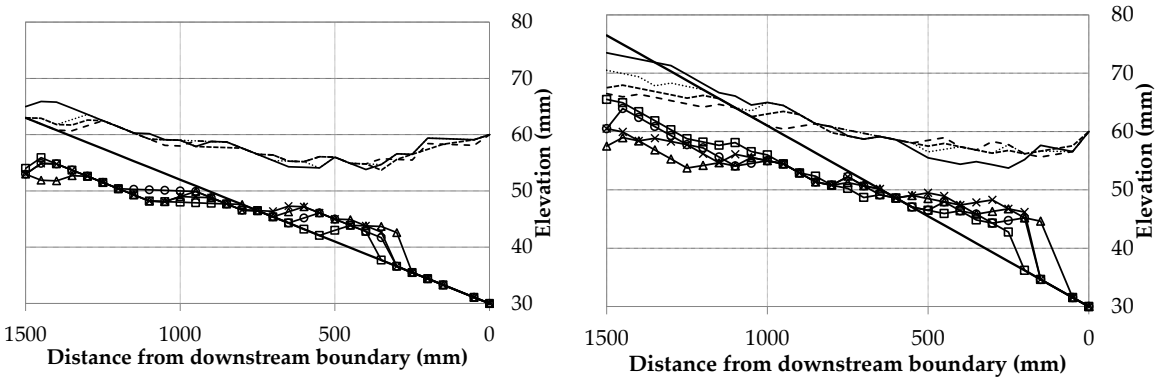

Figure 9. Comparison of delta deposition of SC-I experiments with d_{50}= 1.20 mm.

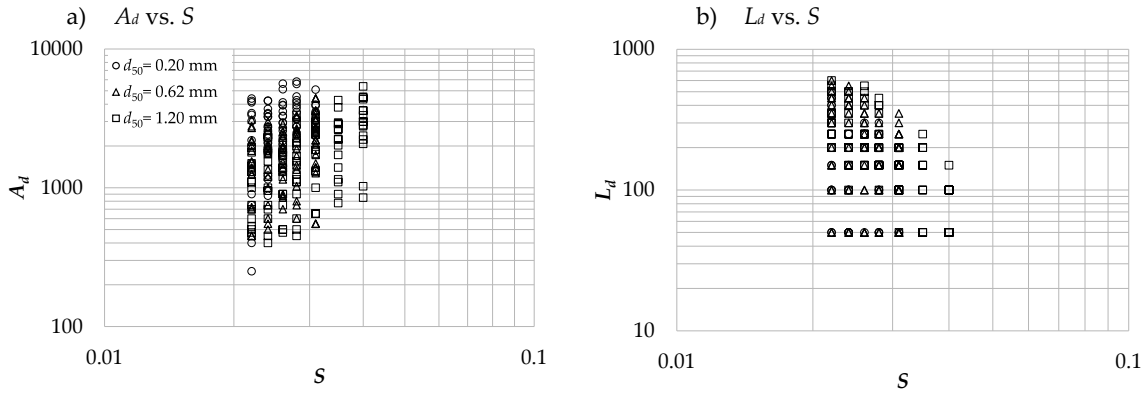

Figure 10. Relationship between deposition rridge properties (volume and length) and channel slope.

Changes in bed elevation and water depth by time step and experimental condition of the SC-II experiment are shown in Figure 10. In the case of A_d, it was proportional to flow rate and riverbed slope, similar to the SC-I experiment results. In addition, when the flow rate is fixed at 6 l/sec, the sedimentation amount at 1 minute after the start of the experiment is 3.27 times that of 9 minutes when the riverbed slope is 1.4%, but 4.53 times at 2.0%. With an increase of 0.6%, the sediment amount increased by about 140%. Comparing the bed slope and water depth graphs in Figure 9 c) and d) of the experimental results with bed slope of 1.4% and 2.0%, in the experimental condition of 1.4%, the backwater region is about 4.2 m away from the downstream weir body. However, at 2.0%, the backwater region is generated with a length of 2.4 m, making the backwater region shorter by about 40%. L_d, the distance from the downstream weir body to the reservoir start point, tended to decrease by 50% as the slope of flume increased from 1.4% to 2.0%.

4.2. Derivation of empirical equation

The correlation analysis between A_d/qt and dimensionless parameters is shown in Figure 11 with the regression curves. To find the parameters with the highest correlation with A_d/qt. Statistical analysis was performed in Table 2. As a result, dimensionless unit stream power, Shields parameter, U^*/ω, and D/d_{50} were analyzed to have the highest correlation. In this study, a nonlinear multiple regression method was applied to develop an empirical equation that can be used to predict the sedimentation behavior of upstream reservoirs. The 288 experimental result data calculated through SC-I cases were randomly classified into 192 and 96 terms for derivation and verification of empirical equation. In addition, in order to understand the statistical characteristics of the two data set, the range, median, and quartile values of VS/ω, A_d/qt, and τ^* for each term were analyzed and presented in Table 3.

Preprints (www.preprints.org) | NOT PEER-REVIEWED | Posted: 8 November 2023 doi:10.20944/preprints202311.0498.v1

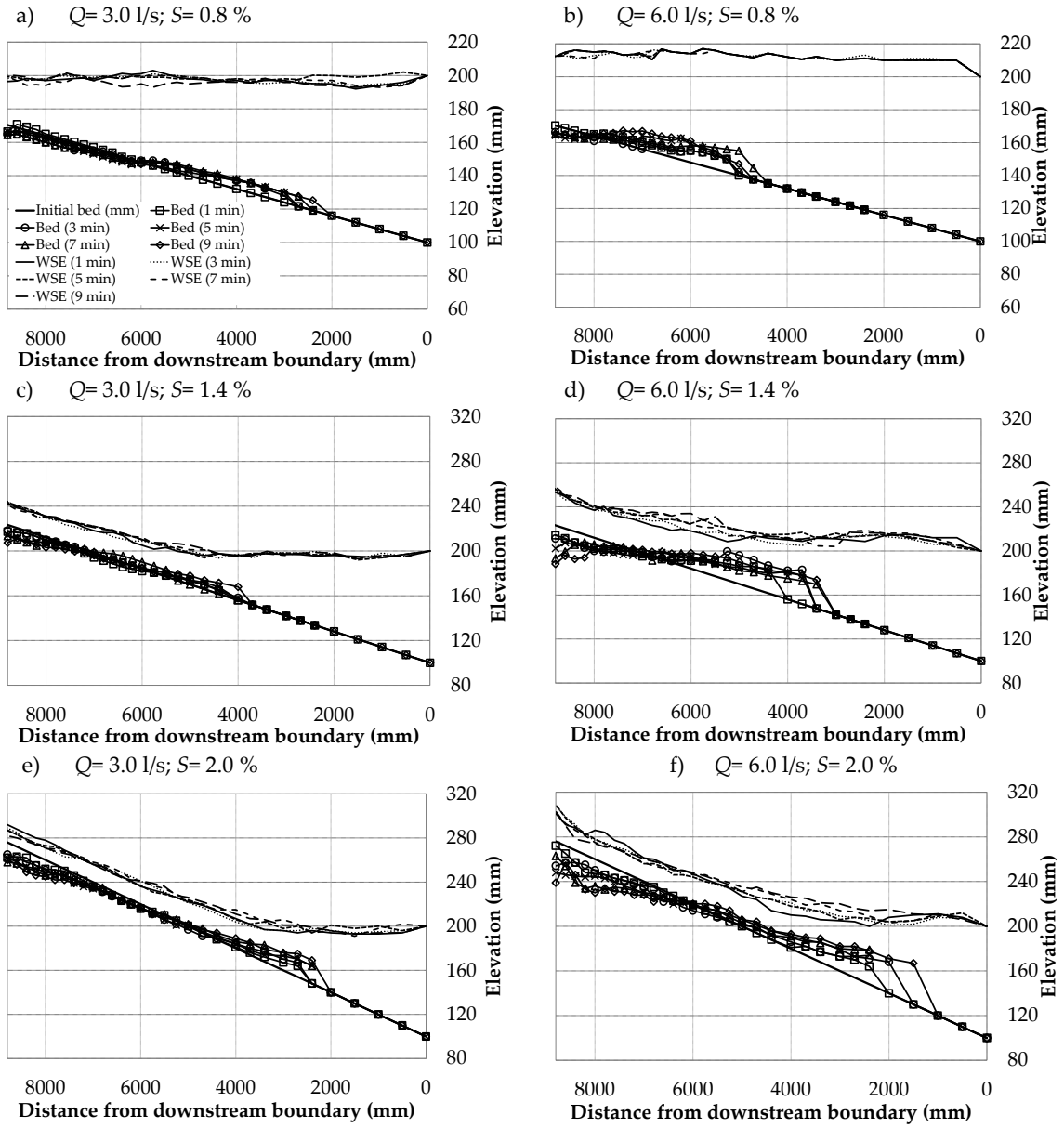

Figure 11. Delta deposition of SC-II experiments (d_{50}= 0.62 mm; h= 100 mm).

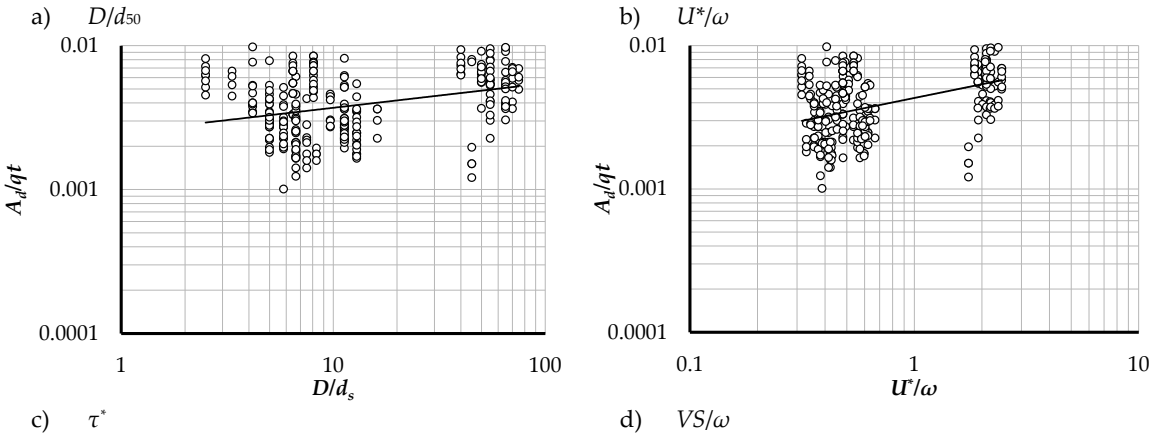

Preprints (www.preprints.org) | NOT PEER-REVIEWED | Posted: 8 November 2023 doi:10.20944/preprints202311.0498.v1

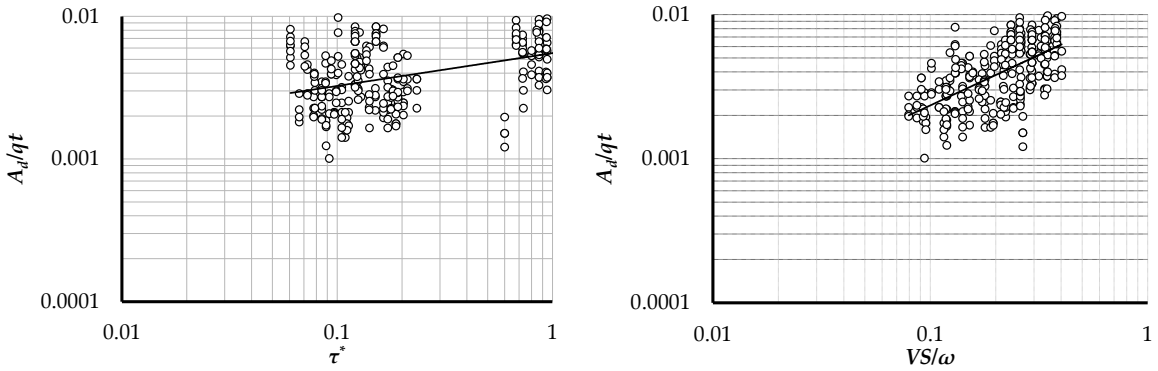

Figure 12. Relationship between A_d/qt and dimensionless hydraulic parameters.

Table 2. Comparison of R^2 between numerical modeling and experimental research for parameters.

Parameter	D/d_s	U^*/ω	τ^*/ω	VS/ω
Numerical Simulation	0.8854	0.9042	0.9052	0.9451
SC-I Experiments	0.1081	0.2002	0.2110	0.3743

Table 3. Statistical characteristics of data sets (SC-I Experiments).

Parameter	Derivation Data Set			Verification Data Set		
	Range	Mean	Quartile	Range	Mean	Quartile
A_d/qt	0.0015-0.0142	0.0039	0.0025	0.0027-0.0085	0.0036	0.0028
VS/ω	0.0796-0.4024	0.2200	0.1307	0.1392-0.3356	0.2176	0.1720
τ^*	0.6000-1.1879	0.1225	0.0888	0.1290-0.2346	0.1681	0.1350

The empirical equation as a result of deriving the multiple regression analysis equation using 192 experimental result data among the SC-I experiment data is as follows:

$$\frac{A_d}{qt} = 0.024\left(\frac{VS}{\omega}\right)^{1.111}(\tau^*)^{0.049} \tag{23}$$

In the derivation of this equation, the correlation coefficient was analyzed to be 0.91 and the standard deviation was 0.00071.

The empirical equation derived in this study was verified using 96 data out of 288 SC-I experiment results and 30 data acquired from SC-II experiment. Figure 13 showed the discrepancy ratio, where the correlation can be seen through a 1:1 graph between the computed results calculated using Equation (23) and the measured data.

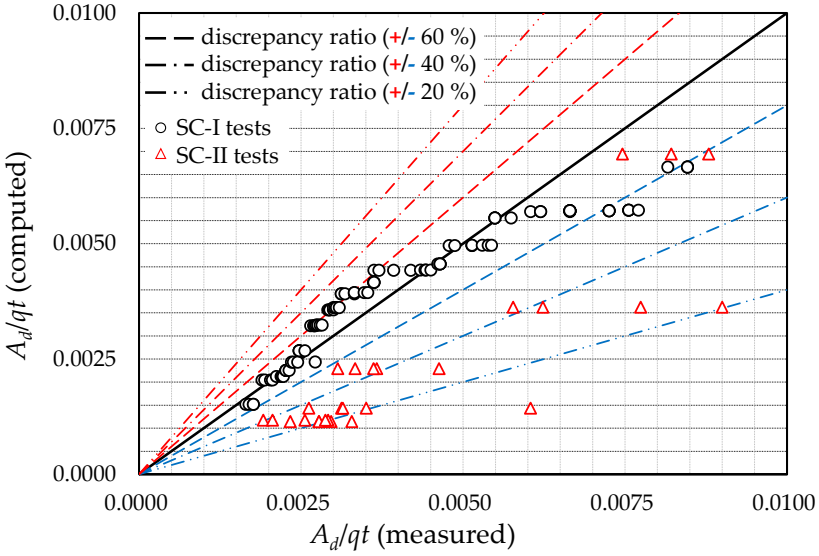

Figure 13. Comparison between measured and computed results.

Preprints (www.preprints.org) | NOT PEER-REVIEWED | Posted: 8 November 2023 doi:10.20944/preprints202311.0498.v1

Figure 14 shows the discrepancy rates for the SC-I experiment and SC-II experiment, respectively. RMSE (Root Mean Square Error), MAE (Mean Absolute Error), and AGD (Averaged Geometric Deviation) were calculated, and the results are shown in Table 4. The SC-I data showed a smaller error than the SC-II data, and it was found that the SC-II experimental conditions were under-predicted with the empirical equation.

$$\mathrm{RMSE} = \left[\sum_{j=1}^{J} \left(Z_{cj} - Z_{mj}\right)^2 / J\right]^{1/2} \tag{23}$$

$$\mathrm{MAE} = \frac{1}{J}\sum_{j=1}^{J} \left|Z_{cj} - Z_{mj}\right| \tag{24}$$

$$\mathrm{AGD} = \left[\prod_{j=1}^{J} R_j\right]^{1/J}, R_j \begin{bmatrix} Z_{cj}/Z_{mj} & Z_{cj} \geq Z_{mj} \\ Z_{mj}/Z_{cj} \text{ for } & Z_{mj} \leq Z_{cj} \end{bmatrix} \tag{25}$$

Herein, Z_c represents the dimensionless sediment deposition calculated using the empirical equation, while Z_m represents the dimensionless sediment deposition measured through experiments. J denotes the number of experiments, and R_j represents the special discrepancy ratio. The verification results are presented in Table 4 and are derived from the analysis of the Pearson correlation coefficient. Accordingly, it was determined that there was a strong positive correlation.

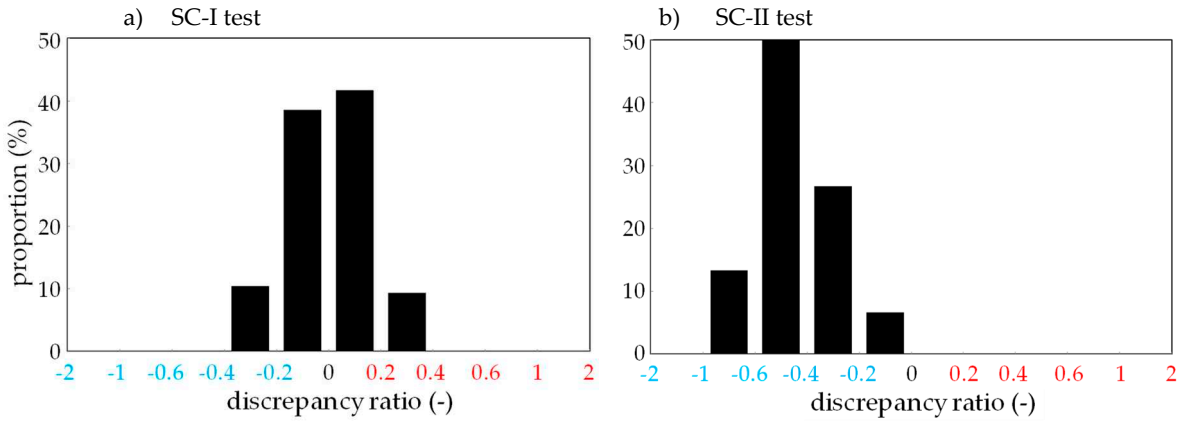

Figure 14. Discrepancy ratios for two data sets.

Table 4. Statistical analysis for verification results.

Experimental Case	Data Set	RMSE	MAE	AGD
SC-I test	96	0.0007	0.0005	1.0390
SC-II test	30	0.0039	0.0026	1.1161

5. Conclusions and discussion

In this study, numerical analysis and mobile bed experiments were performed to investigate the behavior of reservoir delta deposited upstream of weir model. Using the one-dimensional uncoupled numerical approach for the calculation of flow and sediment transport, six dominant factors of the laboratory experiment including dimensionless unit stream power, Shields parameter, ratio of shear velocity and fall velocity, ratio of upstream normal depth and sediment particle size were determined.

From the experimental approach, it was observed that the formation and evolution of a reservoir delta are significantly influenced by four key factors: sediment particle size, channel slope, flow discharge, and downstream water depth. In particular, as the channel slope increased by 0.1%, the sediment deposition increased by approximately 12%. This was confirmed through both experimental results and predictions based on empirical equations. Under the experimental conditions with a channel slope of 0.8%, there was no backwater observed. However, at a channel

Preprints (www.preprints.org) | NOT PEER-REVIEWED | Posted: 8 November 2023 doi:10.20944/preprints202311.0498.v1

slope of 1.4%, backwater was generated, extending approximately 4.2 m. As the channel slope increased to 2.0%, the length of backwater tended to decrease by about 2.6 m. Nevertheless, when the water depth, which maintained a slope nearly parallel to the channel bed, encountered the backwater section, the slope abruptly decreased to nearly 0%, resulting in a rapid reduction of flow and subsequent sedimentation as previously revealed [30].

As a result of one-dimensional numerical simulation, reservoir delta was found to be significantly influenced by four conditions: diameter of sediment particle, bed slope, inlet discharge, and water depth at downstream. Correlation analysis of dimensionless sediment deposition per unit width (A_d/qt) and dimensionless hydraulic and sediment parameters (time, flow rate, fall velocity of sediment particle, unit stream power, water depth at the weir gate, friction velocity, bed slope) Through this, multiple regression equations consisting of dimensionless unit stream power and Shields parameter, which have the greatest correlation, were derived. As a result of statistical analysis through application of the derived empirical formula, RMSE was 0.0007, MAE was 0.0005, and AGD was 1.0390, indicating that the range was quite acceptable.

In particular, sedimentation patterns were observed to differ according to the experimental conditions when there was significant variation in water depth. Therefore, additional research is deemed necessary to address issues related to reservoir capacity and potential degradation of flood stages. On the other hand, it was found that bed elevation changes, which vary with flow, including shear velocity, Shields parameter, and unit stream power based on channel slope and flow discharge in natural rivers, are suitable for the development of reservoir deltas. As a result of predicting the sedimentation amount in experiments using the developed empirical formula, there was a tendency for the predicted sedimentation amount to be somewhat lower than that observed in the smaller scaled experiments (SC-I experiment). This phenomenon can be improved through further research that considers changes in inlet discharge, sediment particle size, and downstream water depth using medium- to large-scale experimental channels.

The empirical formula developed in this study can be employed in two future directions. Firstly, it can be applied for multi-purpose weirs and dams planned for construction in upcoming reservoir projects to predict short- and long-term sedimentation volumes in advance. This information can be utilized to plan for reservoir capacity and sedimentation management. Additionally, it can provide valuable insights into the limitations, dimensions, and requirements for related additional structures when constructing riverine hydraulic facilities. Notably, the empirical formula's application can substitute the need for time-consuming and labor-intensive long-term researches or field measurements when determining deposition in the reservoir delta, suggesting the possibility of using it for the delta deposition management and flushing.

Secondly, the hydraulic similitude applied in this study can contribute to establishing experimental conditions for hydraulic experimental modeling. This will be beneficial for studying long-term deposition and flushing operation management methods in the future. Unlike fixed bed modeling, it is expected that similitude can be more easily achieved by using the method described in this paper for mobile bed modeling, where applying similitude is typically challenging.

Author Contributions: A.J. was responsible for conceptualization, methodology and software application of this research. A.J. and S.W.P. were involved in model validation, data curation and writing—original draft preparation. S.W.P. and C.G.S. were involved in writing—review and editing. C.G.S. contributed to supervision, project administration and funding acquisition. All authors have read and agreed to the published version of the manuscript.

Acknowledgments: This study was supported by Korea Environment Industry & Technology Institute (KEITI) through Environmental R&D Project on the Disaster Prevention of Environmental Facilities, funded by Korea Ministry of Environment (MOE) (2022002850001).

Conflicts of Interest: The authors declare no conflict of interest.

Preprints (www.preprints.org) | NOT PEER-REVIEWED | Posted: 8 November 2023 doi:10.20944/preprints202311.0498.v1

References

1. Morris, G. L.; Fan, J. *Reservoir sedimentation handbook: Design and management of dams, reservoirs, and watersheds for sustainable use*. McGraw-Hill, **1997**, New York, USA: https://doi.org/10.1061/(ASCE)0733-9429(2000)126:6(481).
2. Anton, J. S.; Mário, J. F.; Carmelo, J.; Giovanni, D. C. Reservoir sedimentation, *Journal of Hydraulic Research*, **2016**, 54(6), 595-614. https://doi.org/10.1080/00221686.2016.1225320
3. Julien, P. Y. *Erosion and sedimentation*. Cambridge University Press, **1995**, NY, USA. https://doi.org/10.1017/CBO9780511806049
4. White, R. *Evacuation of sediments from reservoirs*, Thomas Telford Publishing, **2001**, London, UK. http://doi.org/10.1680/eosfr.29538
5. Toniolo, H.; Parker, G. 1D numerical modeling of reservoir sedimentation, *Proceedings IAHR Symposium on River*, Coastal and Estuarine Morphodynamics, Barcelona, Spain, 1-5 September **2003**.
6. Wright, L. D.; Coleman, J. M. Mississippi river mouth processes: Effluent dynamics and morphologic development, *The Journal of Geology*, **1974**, 82(6), 751-778. https://doi.org/10.1086/628028
7. Soni, J. P.; Ranga Raju, K. G.; Garde, R. J. Aggradation in streams due to overloading. *Journal of the Hydraulics Division*, **1980**, 106(1), 117-132. https://doi.org/10.1061/JYCEAJ.0005338
8. Hotchkiss, R. *Reservoir sedimentation and sluicing: experimental and numerical analysis*, University of Minnesota, Project Report, **1990**, No. 304. https://hdl.handle.net/11299/108511
9. Hotchkiss, R. H.; Parker, G. Shock fitting of aggradational profiles due to backwater, *Journal of Hydraulic Engineering*, ASCE, **1991**, 117(9), 1129-1144. https://doi.org/10.1061/(ASCE)0733-9429(1991)117:9(1129)
10. Yang, C.T.; Simões, F.J.M. GSTARS Computer Models and Their Application, part I: Theoretical Development, *International Journal of Sediment Research*, **2008**, 23(3), 197-211. https://doi.org/10.1016/S1001-6279(08)60019-0
11. Simões, F.J.M.; Yang, C.T. GSTARS Computer Models and Their Applications, Part II: Applications. *International Journal of Sediment Research*, **2008**, 23(4), 299-315. https://doi.org/10.1016/S1001-6279(09)60002-0
12. Yang, C.T. Discussion of "Sediment Transport Modeling Review – Current and Future Developments" by A.N. Papanicolaou, M. Elhakeem, G. Krallis, S. Prakash, and J. Edinger. *Journal of Hydraulic Engineering*, ASCE, **2010**, 136(8), 552-555. https://doi.org/10.1061/(ASCE)HY.1943-7900.0000014
13. Fan, J.; Morris, G. L. Reservoir sedimentation I: Delta and density current deposits. *Journal of Hydraulic Engineering*, **1992**, 118(3), 354-369. https://doi.org/10.1061/(ASCE)0733-9429(1992)118:3(354).
14. Fan, J.; Morris, G. L. Reservoir sedimentation II: Reservoir desiltation and long-term storage capacity. *Journal of Hydraulic Engineering*, **1992**, 118(3), 370-384. https://doi.org/10.1061/(ASCE)0733-9429(1992)118:3(370)
15. Ahn, J.; Yang, C. T.; Boyd, P. M.; Pridal, D. B.; Remus, J. I. Numerical modeling of sediment flushing, from Lewis and Clark Lake, *International Journal of Sediment Research*, **2013**, 28(2), 182-193. http://doi.org/10.1016/S1001-6279(13)60030-X
16. Choi, H. *Experimental Investigation of Sedimentation at Multi-purposed Weir*, Master Thesis, Seoul National University, South Korea (in Korean), Feb **2014**. https://snu-primo.hosted.exlibrisgroup.com/permalink/f/1l6eo7m/82SNU_INST21443498980002591
17. Kantoush, S. A.; Bollaert, E; Schleiss, A. S. Experimental and numerical modelling of sedimentation in a rectangular shallow basin, *International Journal of Sediment Research*, **2008**, 23(3), 212-232. https://doi.org/10.1016/S1001-6279(08)60020-7
18. Gökçen, B.; Güney, M. S. Experimental investigation of sediment transport in steady flows, *Scientific Research and Essays*, **2008**, 5(6), 582-591.
19. Matthieu, D.; Benjamin, J; *Sébastien E. Flow and Sediment Deposition in Rectangular Shallow Reservoirs*, Novatech, **2010**. https://hal.science/hal-03296708
20. Souza, L.B.S.; Schulz, H.E.; Villela, S.M.; Gulliver, J.S. Experimental study and numerical simulation of sediment transport in a shallow reservoir, *Journal of Applied Fluid Mechanics*, **2010**, 3(2), 9-21. http://doi.org/10.36884/jafm.3.02.11884
21. Bui, V.H.; Bui, M.D.; Rutschmann, P. Advanced Numerical Modeling of Sediment Transport in Gravel-Bed Rivers. *Water*, **2019**, 11, 550. https://doi.org/10.3390/w11030550
22. Latif, S.D.; Chong, K.L.; Ahmed, A.N. Sediment load prediction in Johor river: deep learning versus machine learning models. *Applied Water Science*, **2023**, 13(79). https://doi.org/10.1007/s13201-023-01874-w
23. Legowo, S.; Hadihardaja, I. K.; Azmeri, A. Estimation of Bank Erosion Due to Reservoir Operation in Cascade (Case Study: Citarum Cascade Reservoir), *Journal of Engineering and Technological Sciences*, **2013**, 41(2), 148-166. https://doi.org/10.5614/itbj.eng.sci.2009.41.2.5
24. Yang, C. T. Unit stream power equations for total load, *Journal of Hydrology*, **1979**, 40, 123-138. https://doi.org/10.1016/0022-1694(79)90092-1
25. Shields, A. *Application of Similarity Principles and Turbulence Research to Bed-Load Movement*, **1936**, California Institute of Technology, Pasadena (Translated from German).

Preprints (www.preprints.org) | NOT PEER-REVIEWED | Posted: 8 November 2023 doi:10.20944/preprints202311.0498.v1

26. Engelund, F. and Hansen, E. *A monograph on sediment transport in alluvial streams*, **1967**, TEKNISKFORLAG Skelbrekgade 4 Copenhagen V, Denmark. http://resolver.tudelft.nl/uuid:81101b08-04b5-4082-9121-861949c336c9
27. Exner, F. M. Über die wechselwirkung zwischen wasser und geschiebe in flüssen, *Sitzungsberichte der Akademie der Wissenschaften Mathematisch-Naturwissenschaftliche Klasse*, **1925**, 134(2a), 165–203.
28. Yang, C. T. Incipient Motion and Sediment Transport, *Journal of the Hydraulics Division*, **1973**, 99(10), 1679-1704. https://doi.org/10.1061/JYCEAJ.0003766
29. Park, S.W.; Hwang, J.H.; Ahn, J. Physical Modeling of Spatial and Temporal Development of Local Scour at the Downstream of Bed Protection for Low Froude Number, *Water* **2019**, 11, 1041. https://doi.org/10.3390/w11051041
30. Wang, L.; Cuthbertson, A.; Pender, G.; Zhong, D. Bed load sediment transport and morphological evolution in a degrading uniform sediment channel under unsteady flow hydrographs, *Water Resources Research*, **2019**, 55, 5431–5452. https://doi.org/10.1029/2018WR024413

Disclaimer/Publisher's Note: The statements, opinions and data contained in all publications are solely those of the individual author(s) and contributor(s) and not of MDPI and/or the editor(s). MDPI and/or the editor(s) disclaim responsibility for any injury to people or property resulting from any ideas, methods, instructions or products referred to in the content.